ELSEVIER

Neurobiology of Disease

www.elsevier.com/locate/ynbdi
Neurobiology of Disease 17 (2004) 290–299

Expression analysis of the N-Myc downstream-regulated gene 1 indicates that myelinating Schwann cells are the primary disease target in hereditary motor and sensory neuropathy-Lom

Philipp Berger,[a] Erich E. Sirkowski,[b] Steven S. Scherer,[b,1] and Ueli Suter[a,*,1]

[a]*Department of Biology, Institute of Cell Biology, Swiss Federal Institute of Technology, ETH-Hönggerberg, CH-8093 Zürich, Switzerland*
[b]*Department of Neurology, The University of Pennsylvania Medical Center, Philadelphia, PA 19104-6146, USA*

Received 26 November 2003; revised 27 April 2004; accepted 9 July 2004

Mutations in the gene encoding N-myc downstream-regulated gene-1 (*NDRG1*) lead to truncations of the encoded protein and are associated with an autosomal recessive demyelinating neuropathy—hereditary motor and sensory neuropathy-Lom. NDRG1 protein is highly expressed in peripheral nerve and is localized in the cytoplasm of myelinating Schwann cells, including the paranodes and Schmidt–Lanterman incisures. In contrast, sensory and motor neurons as well as their axons lack NDRG1. NDRG1 mRNA levels in developing and injured adult sciatic nerves parallel those of myelin-related genes, indicating that the expression of NDRG1 in myelinating Schwann cells is regulated by axonal interactions. Oligodendrocytes also express NDRG1, and the subtle CNS deficits of affected patients may result from a lack of NDRG1 in these cells. Our data predict that the loss of NDRG1 leads to a Schwann cell autonomous phenotype resulting in demyelination, with secondary axonal loss.

Keywords: Neuropathy; Oligodendrocytes; Myelin; Charcot-Marie-Tooth disease; CMT; Schwann cells

Introduction

Hereditary motor and sensory neuropathy (HMSN), also called Charcot–Marie–Tooth (CMT) disease, is a common but heterogeneous group of disorders (Dyck et al., 1993). CMT or HMSN are subdivided into demyelinating and axonal forms (Berger et al., 2002a; Dyck and Lambert, 1968a,b; Kleopa and Scherer, 2002). These can be further subdivided in autosomal dominant demyelinating (CMT1), recessive demyelinating (CMT4), dominant axonal (CMT2), and recessive axonal forms (AR-CMT2 or CMT2B). Furthermore, X-linked forms of CMT (CMTX) are relatively frequent. In the last decade, the genes responsible for the most frequent forms of CMT have been identified (Suter and Scherer, 2003), but the origins of many rarer forms are still undiscovered (Boerkoel et al., 2002).

Autosomal recessive mutations in the N-myc downstream-regulated gene 1 (*NDRG1*) cause HMSN-Lom (HMSNL, also called CMT4D) (Kalaydjieva et al., 1996, 1998, 2000). CMT4D was first described in a Gypsy community near Lom (Bulgaria) but has been subsequently found in other Gypsy communities throughout Europe. The clinical phenotype of CMT4D becomes apparent in the first decade of life, with distal leg weakness causing a gait disorder, followed by upper limb weakness in the second decade, and deafness in the third decade. Skeletal deformities are also frequently observed. CMT4D has been classified as demyelinating neuropathy because nerve conduction velocities are severely slowed and nerve biopsies show evidence of demyelination and remyelination. Severe axonal loss is unusually pronounced in young patients and appears to be progressive (Baethmann et al., 1998; Butinar et al., 1999; Kalaydjieva et al., 1998; Merlini et al., 1998).

Little is known about NDRG1 itself. Besides being repressed by N-myc during mouse development (Shimono et al., 1999), it is up-regulated during cellular differentiation (van Belzen et al., 1997) by reducing agents and tunicamycin (Kokame et al., 1996), Ni^{2+} (Zhou et al., 1998), and other chemical agents (Piquemal et al., 1999; Ulrix et al., 1999). NDRG1 is positively regulated by p53, leading to reduced expression in p53-dependent tumors (Kurdistani et al., 1998), and has been proposed as a metastasis suppressor gene (Bandyopadhyay et al., 2003; Guan et al., 2000). The molecular function of NDRG1 is also enigmatic. It belongs to the superfamily of α/β hydrolases, but the crucial catalytic residues are not present (Shaw et al., 2002). NDRG1 contains a putative phosphopantetheine binding site (Kokame et al., 1996) and a 3× repeated 10 amino acid sequence at the C-terminus that

* Corresponding author. Institute of Cell Biology, ETH Hönggerberg, CH-8093 Zürich, Switzerland. Fax: +41 1 633 1190.
E-mail address: usuter@cell.biol.ethz.ch (U. Suter).
[1] These authors contributed equally to this work.
Available online on ScienceDirect (www.sciencedirect.com.)

0969-9961/$ - see front matter © 2004 Elsevier Inc. All rights reserved.
doi:10.1016/j.nbd.2004.07.014

is probably involved in the binding of Ni^{2+} and Cu^{2+} ions (Zoroddu et al., 2001). NDRG1 has also been proposed to function in the endoplasmic reticulum stress response (Segawa et al., 2002).

In contrast to the above ideas, the limited clinical phenotype of CMT4D patients indicates that NDRG1 plays mainly a crucial function in the development and/or maintenance of peripheral nerves. Thus, we have examined the expression of NDRG1 in the PNS. NDRG1 is expressed by myelinating Schwann cells, and its expression is modulated like that of myelin-related genes in both developing and injured nerves. NDRG1 is not found in sensory or motor neurons. Thus, the primary defect of CMT4D resides in defective myelinating Schwann cells, which in turn have profound effects on the integrity of their associated axons, as indicated by the severe axonal loss observed in the disease (Suter and Scherer, 2003).

Materials and methods

Constructs for NDRG1 expression and production of NDRG1 antiserum

The NDRG1 cDNA was obtained by RT-PCR from mouse sciatic nerve RNA using the primers NDRG1-ATGBam (5′-CAC GGA AGG ATC CCG AGA GCT ACA TGA CGT GGA C-3′) and NDRG1-StoPst (5′-ATG CAC CTG CAG CTT AGC AGG ACA CCT CCA TGG AC-3′). The sequence of the coding region was identical to known NCBI database entries (*NM_010884*). For eukaryotic expression, the *Bam*HI/*Pst*I cut cDNA was cloned into the pcDNA3.1 vector (Invitrogen). For prokaryotic expression with a N-terminal His(6) tag, the cDNA corresponding to amino acids 2–394 was cloned into the *Bam*HI/*Pst*I cut pQE30 vector (Qiagen). Recombinant NDRG1 protein for immunization was produced in *Escherichia coli* XL1-blue cells and the protein was purified using standard procedures (Qiagen). This protein was then used for the immunization of rabbits (Institut für Labortierkunde, University of Zürich).

Transfection of cells

Rat Schwann cells were isolated and cultured as previously described (Taylor et al., 1995). Rat Schwann cells and COS7 cells were transfected with the eukaryotic expression vector pcDNA3.1-NDRG1 (see above) using either FuGENE6 (Roche) or Superfect (Qiagen) according to manufacturers recommendations. Forty hours after transfection, cells were fixed with 2% paraformaldehyde and then blocked with 10% FCS/0.05% saponin/PBS. Antibodies were diluted as follows in blocking solution: mouse anti-LBPA (1:100; kindly provided by Dr. J. Gruenberg, Geneva), mouse anti-PDI ID3 (1:100; kindly provided by Dr. S Fuller, Heidelberg), and mouse anti-giantin (1:100; kindly provided by Dr. H.P. Hauri, Basel). The ubiquitin staining was performed in cells transfected with a C-terminally VSV-tagged NDRG1 construct and stained with a mouse anti-VSV-G (1:100; P5D4, Roche) and a rabbit anti-ubiquitin antibody (1:50; kindly provided by Dr. E. Ehler, Zürich). Appropriate FITC- and TRITC-conjugated secondary antisera were used for visualization. Lysosomes and mitochondria were stained using Lysotracker or Mitotracker according to manufacturers recommendations before fixation (Molecular Probes).

Surgery and collection of tissues

Using aseptic technique, the sciatic nerves of anesthetized (50 mg/kg pentobarbital ip), adult (10–13 week old) Sprague–Dawley rats were exposed at the sciatic notch. Permanent axotomy was accomplished by doubly ligating nerves, transecting between the ligatures with iridectomy scissors, and suturing the two nerve stumps so they were at least 1 cm apart; this technique prevents axonal regeneration to the distal nerve stump for at least 2

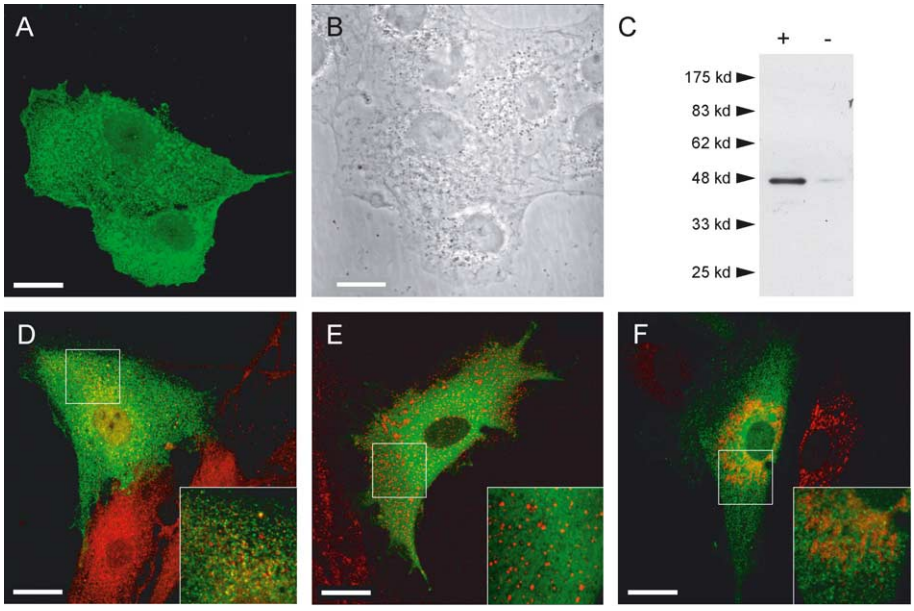

Fig. 1. Transient expression of NDRG1 in transfected cells. (A) NDRG1-transfected COS cells stained with a rabbit antiserum against NDRG1 (green); phase image (B). (C) Western blot analysis of NDRG1-transfected COS cells (+), showing a single band of NDRG1. (−) Untransfected COS cells. (D–F) NDRG1-tranfected Schwann cells doubly labeled for NDRG1 (green) and (D) ubiquitin, (E) LBPA (for late endosomes), or (F) PDI (for the endoplasmic reticulum). Scale bars: 20 μm.

months. Nerve crush was produced by tightly compressing the sciatic nerve at the sciatic notch with flattened forceps twice, each time for 10 s; this method causes all of the axons to degenerate but allows axonal regeneration. At various times after nerve injury, the animals were sacrificed by CO_2 inhalation, the distal nerve stumps were removed, and the most proximal 2–3 mm were trimmed off. For transected nerves, the entire distal nerve stump was taken from just below the lesion to the ankle (about 4 cm). For crushed nerves, the distal nerve stump was divided into two equal segments, termed the proximal and distal segments, each about 2 cm long. The nerves were immediately frozen in liquid nitrogen and stored at −80°C. All animal protocols were approved by the Institutional Animal Care and Use Committee of the University of Pennsylvania.

Northern blot and quantitative RT-PCR analysis

RNA was isolated from rat sciatic nerves and Schwann cells by CsCl gradient centrifugation (Chirgwin et al., 1979) or using Trizol reagent (Invitrogen). Equal amounts (10 μg) of total RNA were electrophoresed in 1% agarose, 2.2 M formaldehyde gels, transferred to nylon membranes (Duralon, Stratagene) in 6× SSC, and UV cross-linked (0.12 joules). Blots were prehybridized, hybridized, and washed using standard techniques; the final stringency of the wash was 0.2× SSC at 65°C for 30 min (Sambrook et al., 1989). The following cDNAs were used as probes: a 1.1-kb fragment of mouse NDRG1, a full-length cDNA of rat P0 (Lemke and Axel, 1985), a 2.0-kb fragment of rat MBP (gift of Dr. J. Kamholz, Detroit), and a full-length cDNA of rat glyceraldehyde 3-phosphate dehydrogenase (GAPDH) (Fort et al., 1985). Plasmid inserts were isolated after restriction endonuclease digestion by agarose gel electrophoresis and purified by electroelution. ^{32}P-labeled cDNA probes with specific activities of 2–5 × 10^9 cpm/μg were prepared by primer extension with random hexamers using the Prim-a-gene kit (Promega) according to the manufacturer's instructions.

Quantitative RT-PCR was carried out on a ABI Prism 7000 Sequence Detection System using TaqMan technology (Applied Biosystems). PCR was performed with the unlabelled primers rNDRG1-for (5′-TTC ACA AGT TTG GGC TTA AGA GTG T-3′) and rNDRG1-back (5′-ATC TCA GGG TTG TTG AGT GCA A-3′) and the 5′ FAM and 3′ TAMRA-labeled primer NDRG1-FAMTAMRA (5′-TCA GGA TGT AGG CGC CAG CTC CTG TCC-3′). The reactions were carried out in triplicates with rat cDNAs as template using TaqMan Universal PCR Master Mix according to the manufacturer's recommendations. The amount of 18 S rRNA was determined in parallel reactions as internal control.

Immunohistochemistry

Nerve fibers were teased from fresh, unfixed nerves, or from nerves that had been fixed for 30 min in 4% paraformaldehyde or Zamboni's fixative. Teased fibers were dried on glass slides, then postfixed for 10 min with acetone. Other sciatic nerves, as well as optic nerves, brains, and spinal cords, were embedded in OCT (Miles, Elkhart, IN) without prior fixation or after fixation in 4% paraformaldehyde. Frozen sections were postfixed for 10 min in acetone. Teased fibers and sections were blocked for at least 1 h in 10% fish skin gelatin containing 0.5% Triton X-100 and incubated 24–48 h at 4°C with the rabbit antiserum against NDRG1, combined with monoclonal antibodies against MAG (1:100; Boehringer-Mannheim, Indianapolis, IN), adenomatous polyposis coli (APC Ab-7; 1:20, Calbiochem), glial fibrillary acidic protein (1:500; Sigma), and neurofilament heavy chain (1:10; Ta51) (Lee et al., 1982). After incubating with the primary antibodies, the sections were washed, then incubated with the appropriate fluorescein-, rhodamine-, and cyano-5-conjugated donkey anti-rabbit, anti-mouse, and anti-rat secondary antibodies (Jackson ImmunoResearch Laboratories, West Grove, PA). Digital images were taken with a Leica DMR microscope equipped with a cooled Hamamatsu camera.

Western blotting

Frozen tissues from adult mice were homogenized using a Polytron PT1200 (Kinematica) in 50 mM Tris–HCl pH 7.5, 100 mM NaCl, 2 mM EDTA, 1% Triton X-100, 2 mM PMSF. Protein extracts were similarly prepared from cultured COS cells after scraping the cells into the same solution. Insoluble material was removed by centrifugation in a microfuge for 3 min at 14,000 rpm, and the concentration of protein in the supernatant was measured with a Biorad DC Assay kit according to the manufacturer's instructions using BSA as standard. Equal amounts (15 μg) of protein were separated on 12.5% acrylamide–0.1% SDS gels, transferred to Immobilon-P PVDF membrane (Millipore), blocked

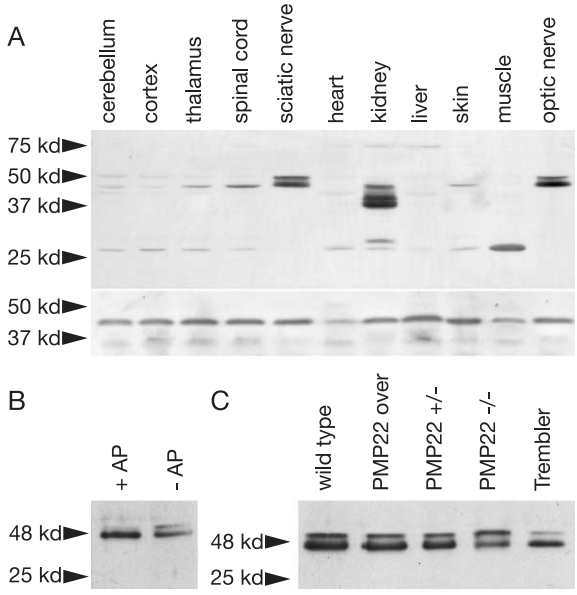

Fig. 2. Immunoblot analysis of NDRG1. (A) Protein levels in different mouse tissues. Each lane contains 15 μg of protein homogenate from the indicated tissues. The blot was first probed with a rabbit NDRG1 antiserum (upper panel), then reprobed with a mouse monoclonal antibody against actin (lower panel). NDRG1 levels were highest in the sciatic and optic nerve, with lower levels in other CNS regions and skin. No expression was detectable in the heart, liver, or skeletal muscle. In the kidney, two strong signals at 35 and 37 kDa were observed in addition to the expected signal at 47 kDa. We did not observe an alternatively spliced mRNA in the Northern blot analysis and none has been described so far (data not shown). Thus, these products might be due to proteolytic cleavage although other explanations cannot be formally excluded. The same applies to the weak 25-kDa band that is present in most tissues. (B) Treatment of sciatic nerve lysates with alkaline phosphatase leads to a single band, indicating that NDRG1 is phosphorylated in this tissue. (C) Sciatic nerve extracts from different PMP22 mutant animals show that the proportion of phosphorylated (upper band) NDRG1 appears reduced in *Tr* animals and slightly increased in *Pmp22*-null animals.

(3% BSA in TBST), then incubated with a rabbit antiserum against NDRG1, diluted 1:4000, for 2 h at room temperature. The membranes were washed with TBST, then incubated at room temperature in peroxidase-coupled goat anti-rabbit immunoglobulin (Santa Cruz Biotechnology), diluted 1:20,000. After 1.5 h, the membranes were washed and developed with chemiluminescence reagent (Perkin Elmer Life Sciences) or chlornaphol. The membranes were reprobed with a monoclonal antibody against actin (diluted 1:1000 in 3% BSA) followed by incubation with alkaline phosphatase-coupled goat-anti-mouse antibodies (1:15,000 in 5% milk powder). The blot was the developed with CDP-Star (Roche). For dephosphorylation of NDRG1, 10 μg protein from sciatic nerve was incubated with 5 U alkaline phosphatase (Roche) for 5 h at 37°.

Results

Myelinating Schwann cells express NDRG1

To characterize the expression of NDRG1 in rodents, we generated a rabbit antiserum against the recombinant protein (see Materials and Methods). The resulting antiserum showed a specific, predominantly cytoplasmic staining in COS7 cells transiently transfected with an expression construct containing full-length mouse NDRG1 (Figs. 1A and B). Western blot analysis of transfected cells revealed a single band of the expected size (Fig. 1C). The weak signal in untransfected cells most likely represents endogenous NDRG1 protein. Cultured rat Schwann cells did not express detectable levels of NDRG1 by immunocytochemistry (data not shown). They were transiently transfected with the NDRG1 expression vector to determine the subcellular distribution of the protein. A diffuse cytosolic staining was observed, similar to the findings in COS7 cells and consistent with earlier reports in other cell types (Kurdistani et al., 1998; Qu et al., 2002). In addition to the cytosolic staining, a more distinct punctate staining was seen in approximately 30% of the transfected cells. We characterized this pattern further by costaining with markers of specific subcellular compartments. A partial overlap with ubiquitin was observed (Fig. 1D), but no overlap was found with markers of late endosomes (LBPA; Fig. 1E), the endoplasmatic reticulum (PDI; Fig. 1F), lysosomes, the Golgi, or mitochondria (data not shown).

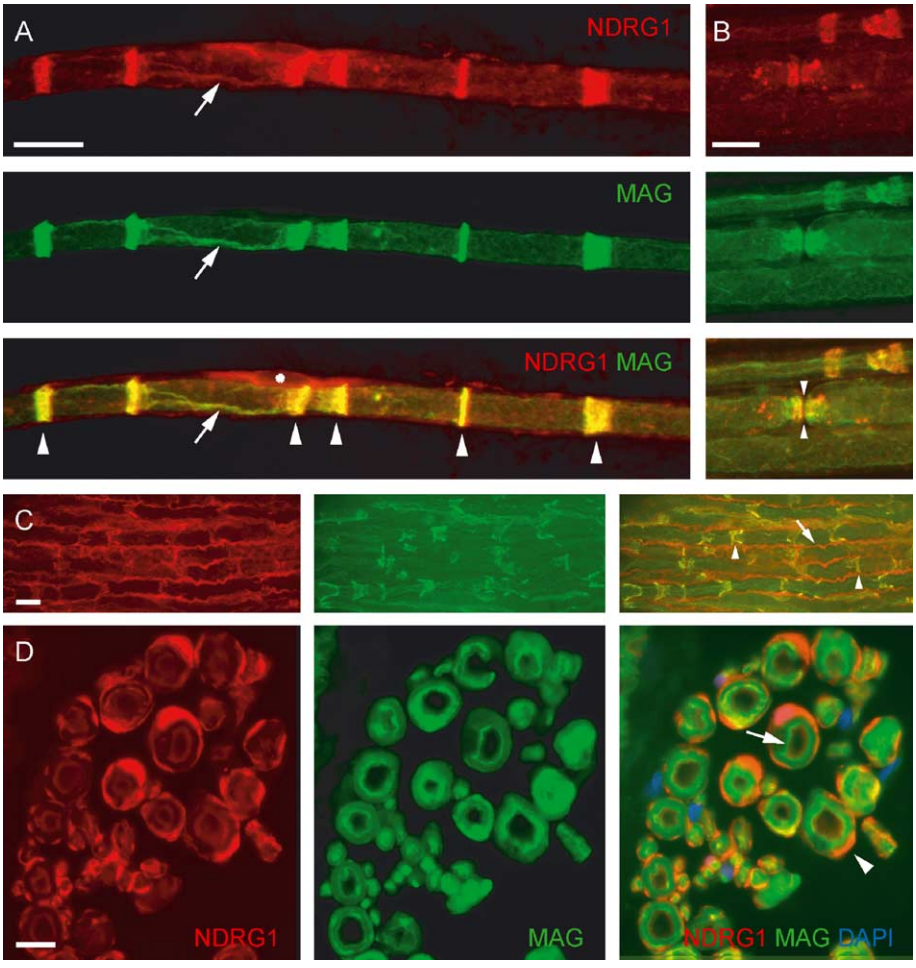

Fig. 3. Localization of NDRG1 in the adult peripheral nerve. (A and B) Fixed teased fibers were double labeled with a rabbit antiserum against NDRG1 (red) and a monoclonal antibody against MAG (green). NDRG1 colocalizes with MAG in incisures (arrowheads), the inner mesaxon (arrow), and in paranodes (the region flanking the nodes; apposed arrowheads). The Schwann cell nucleus is marked with an asterisk. (C) Longitudinal section through the rat sciatic nerve. NDRG1 (red) is mainly localized in the abaxonal cytoplasm (arrow) but colocalizes with MAG (green) in incisures (arrowheads). (D) Transverse section of ventral roots. NDRG1 staining is stronger in the abaxonal cytoplasm (arrowhead) than the MAG staining localized at the innermost myelin membrane (arrow). Scale bars: 10 μm.

To determine the expression of NDRG1 in various tissues, we performed Western blot analysis on adult mouse tissues. Sciatic nerve and optic nerve had particularly high levels (Fig. 2A), appearing as a double band. Because the larger NDRG1 isoform may result from phosphorylation (Agarwala et al., 2000), we treated sciatic nerve lysates with alkaline phosphatase. After treatment, NDRG1 ran as a single 47-kDa band, indicating that the 49-kDa band is indeed phosphorylated NDRG1 (Fig. 2B). To evaluate the possibility that the phosphorylation of NDRG1 can be induced as part of an ER stress response (Agarwala et al., 2000), we examined sciatic nerves from Trembler (*Tr*) mice. These animals carry a dominant *Pmp22* point mutation (Suter et al., 1992) that corresponds to a human mutation that causes a severe demyelinating neuropathy (http://molgen-www.uia.ac.be/CMTMutations/). Because this mutant PMP22 protein is retained in the ER (Naef et al., 1997), we speculated that the phosphorylation of NDRG1 might be affected. Thus, we examined sciatic nerve extracts from *Tr*, as well as wild-type, *Pmp22*-overexpressing (Magyar et al., 1996), and homozygous and heterozygous *Pmp22* knockout mice (Adlkofer et al., 1995, 1997). NDRG1 phosphorylation was not heavily affected but appeared slightly reduced in *Tr* (Fig. 2C).

To determine the cellular distribution of NDRG1 in sciatic nerve, we immunostained teased fibers from adult rats with NDRG1 antiserum and a mouse monoclonal antibody against myelin-associated glycoprotein (MAG). NDRG1 colocalized with MAG in the paranodes, incisures, and the inner mesaxon of myelin sheaths. NDRG1, but not MAG immunoreactivity, was seen in the perinuclear region and abaxonal cytoplasm of myelinating Schwann cells (Figs. 3A and B). To investigate this further, we examined longitudinal and transverse sections of the sciatic nerve and the nerve roots (Figs. 3C and D). In sections, NDRG1 staining of the outer or abaxonal cytoplasm was more apparent, in contrast to the MAG staining of the inner or adaxonal Schwann cell membrane. We also examined *TrJ* mice, which have a missense mutation in *Pmp22* that causes the mutant protein to be retained in the intermediate compartment between the ER and the Golgi (Tobler et al., 1999). Although myelin sheaths are not properly formed in *TrJ* mice—the internodes are short and there are relatively few incisures—abundant NDRG1 immunoreactivity was found in the Schwann cell cytoplasm (Figs. 4A and B). In contrast, there was little NDRG1 staining in Schwann cells that appeared to ensheathe axons without forming a multilamellar myelin sheath (these cells had adaxonal MAG staining but lacked paranodes and incisures) (Figs. 4C and D).

To determine whether NDRG1 is expressed by myelinating Schwann cells in humans, we immunostained sural nerve biopsies that were done for diagnostic purposes from patients who had axonal neuropathies. In three different biopsies, there was NDRG1 immunoreactivity in myelinating Schwann cells, but it was difficult to determine its subcellular localization. Fig. 4E shows an NDRG1-positive teased fiber, and similar results were seen in frozen sections (data not shown). Thus, human myelinating Schwann cells express NDRG1.

For most inherited demyelinating neuropathies, the expectation is that myelinating Schwann cells express the protein encoded by the mutant gene and neuronal expression does not

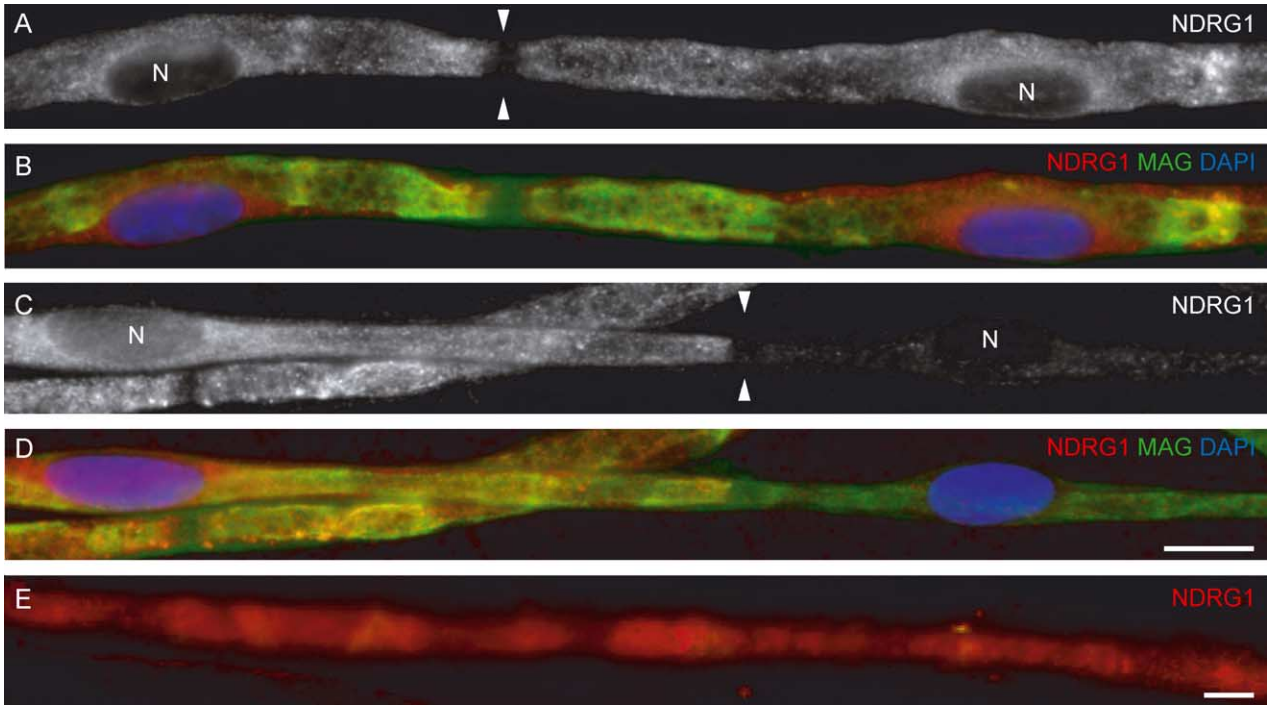

Fig. 4. Myelinating Schwann cells in *Trembler.J* (*TrJ*) mice and humans express NDRG1. These are images of fixed teased fibers from adult *TrJ* mice (A–D) and a human sural nerve biopsy (E), double labeled for NDRG1 (red; B, D, and E) and MAG (green; B and D); DAPI (blue) was used a nuclear counterstain (B and D). In *TrJ* nerves, the myelin sheaths are shorter than normal (A–D), as seen by the short internuclear distances of adjacent Schwann cell nuclei (N), and typically lack well-developed paranodes and incisures. Nevertheless, cytoplasmic NDRG1 immunoreactivity is present. A MAG-positive Schwann cell that appears to ensheathe but not myelinate an axon (the Schwann cell on the right side in C and D), however, has very little NDRG1 immunoreactivity. Apposed arrowheads indicate the positions of nodes. Panel E shows a single teased fiber from a sural nerve human biopsy from a 10-year-old child with an axonal neuropathy. The myelinating Schwann cells are NDRG1 positive. Scale bars: 10 μm.

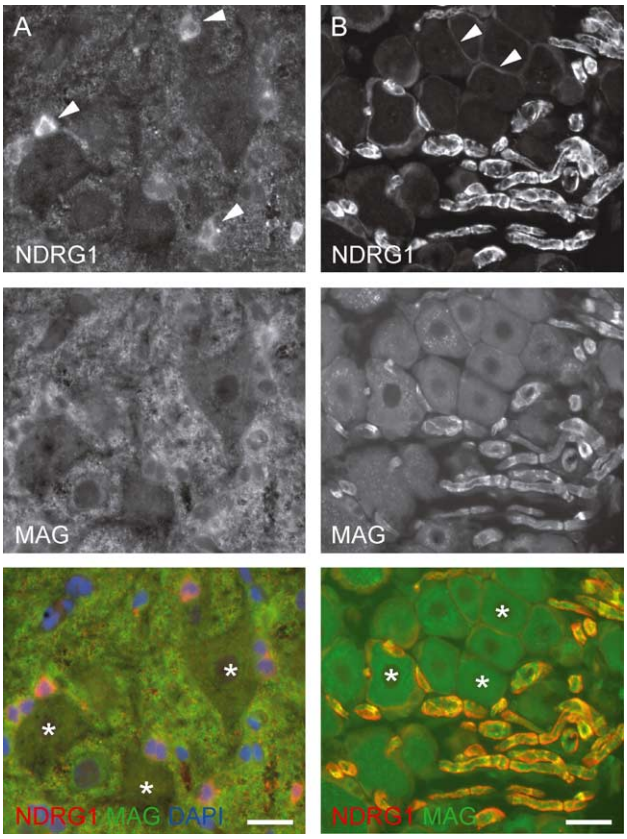

Fig. 5. NDRG1 is not detected in PNS neurons. These are images of sections of the spinal cord (A), dorsal root ganglia (B), double labeled with a rabbit antiserum against NDRG1 (red), and a monoclonal antibody against MAG (green); DAPI nuclear counterstaining (blue) is included in the merged image shown in A. In the spinal cord, NDRG1 is not detected in motor neurons (asterisks); the NDRG1-positive cells (arrowheads) are oligodendrocytes. In the DRG, NDRG1 is not detected in sensory neurons (asterisks); the NDRG1-positive cells are satellite cells (arrowheads) and myelinating Schwann cells. Scale bars: 10 μm.

contribute to the pathogenesis (Suter and Scherer, 2003). However, this view has recently been questioned and in some forms of HMSN/CMT neuronal expression may contribute (Berger et al., 2002a,b; Maier et al., 2002). To address this issue, we examined the expression of NDRG1 in motor and sensory neurons, the sources of myelinated axons in the PNS. As shown in Fig. 5, NDRG1 immunoreactivity was not detected in either type of neurons, although adjacent glial cells were NDRG1 positive.

Axon–Schwann cell interactions regulate NDRG1 expression

Northern blot analysis of human tissues indicated that NDRG1 is widely expressed (Lachat et al., 2002). To investigate this issue further, we performed quantitative RT-PCR of rodent tissues. In the adult rat, the highest NDRG1 mRNA levels were found in the sciatic nerve, followed by kidney, spinal cord, optic nerve, cerebellum, and colon (Fig. 6A). Further, in the developing rat sciatic nerve, a striking parallel between NDRG1 and PMP22 mRNA (Snipes et al., 1992) expression was found (Fig. 6B)—their levels rise sharply soon after birth, remain high throughout the major myelination period (P8-P20), and decline in the adult nerve (P120).

Many myelin-related genes show this pattern of expression in developing nerves. This expression typically depends on the integrity of axon–Schwann cell interactions, which can be experimentally disrupted by nerve injury (Scherer and Salzer, 2001). Thus, we examined the expression of NDRG1 mRNA in adult rat sciatic nerves that were either transected (to cause axonal degeneration and to prevent axonal regeneration) or crushed (to cause axonal degeneration but allow axonal regeneration and hence remyelination of regenerated axons). As shown in Fig. 7A, NDRG1 mRNA levels were strongly reduced distal to the injury by 4 days posttransection and remained low even 2 months later. After nerve crush (Fig. 7B), however, NDRG1 transcript levels also fell initially but returned by 24 days, reaching normal levels after 2 months when remyelination of regenerated axons is complete.

To determine the effect of nerve injury on NDRG1 protein, we examined the distal nerve stumps of adult rat sciatic nerves between 4 and 58 days postlesion. At 4 days posttransection, the myelin sheaths looked largely intact and NDRG1 and MAG stainings resemble that in unlesioned nerves (Fig. 8A). At 12 days, the architecture of most myelin sheaths was obliterated, and there

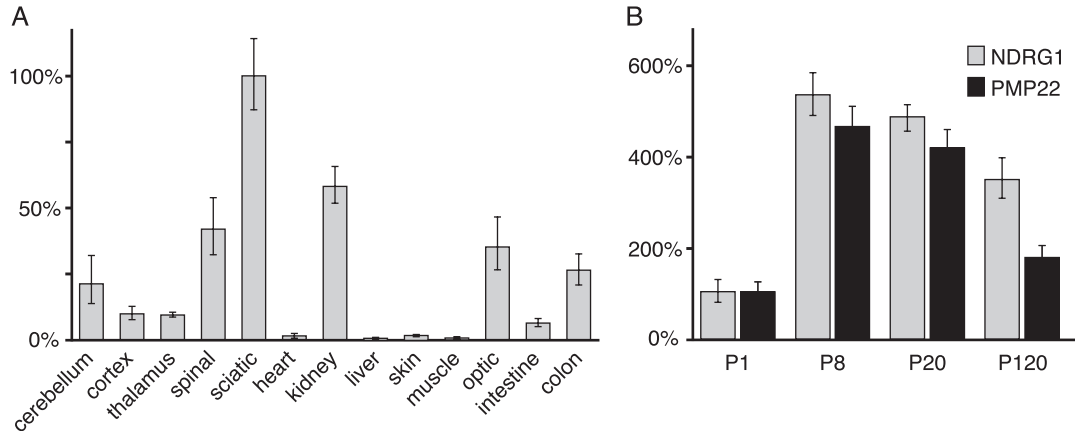

Fig. 6. RT-PCR analysis of NDRG1 mRNA expression in rat tissues. (A) NDRG1 mRNA was detected in all neural tissues and in kidney, intestine, and colon. Used as internal control was 18 S rRNA, and the NDRG1 level in the sciatic nerve was defined as 100%. (B) NDRG1 mRNA expression in the sciatic nerve during development. The NDRG1 expression level is low at birth and highest during the peak of myelination. PMP22 mRNA levels were measured as a control. 18 S rRNA was used as internal control, the P1 levels of each expressed gene were defined as 100%.

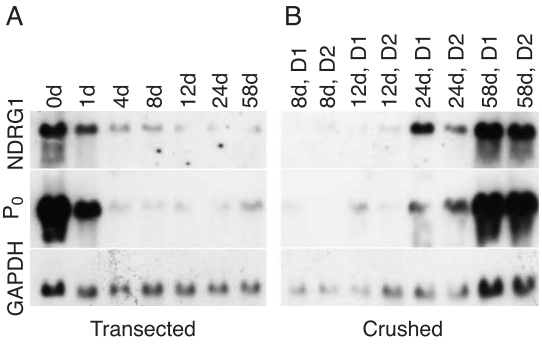

Fig. 7. Expression of NDRG1 mRNA in lesioned adult rat sciatic nerve. Each lane contains 10 μg of total RNA isolated from the distal nerve stumps of adult rat sciatic nerves following transection for the indicated number of days; the "0d" sample is from unlesioned adult nerves. For crushed nerves, the distal stumps were divided into proximal (D1) and distal (D2) segments to illustrate better the proximal-to-distal changes in gene expression that accompany remyelination of regenerated axons. The blots were hybridized together, sequentially, with radiolabeled cDNA probes for NDRG1, GAPDH, and P0 and exposed to film 7 days, 10 days, and 16 h, respectively.

were large blobs of NDRG1- and MAG-immunoreactive material, both in Schwann cells and in macrophages (Fig. 8B). At 58 days, there were small "speckles" of NDRG1 immunoreactivity in Schwann cells and scattered small blobs of MAG immunoreactivity in macrophages (Fig. 8C). These data show that the expression of NDRG1, like that of other myelin-related proteins, decreases after permanent axotomy and that macrophages contribute to the phagocytosis of myelin-related proteins (Scherer and Salzer, 2001). In crushed nerves, NDRG1 immunoreactivity was seen in myelinating Schwann cells around regenerated axons (data not shown).

Oligodendrocytes express NDRG1

Slowing of brainstem auditory evoked potentials (BAEPs) in some CMT4D patients indicates that there may be a subtle CNS defect (Kalaydjieva et al., 1998). To determine the cellular basis of this finding, we immunostained various regions of the rat and mouse CNS, including olfactory bulb, cerebrum, brainstem, cerebellum, optic nerve, and spinal cord. NDRG1 immunoreactivity was most pronounced in the cytoplasm of cells that were found in both the gray and white matter. In the white matter, these cells were often arranged in longitudinal rows parallel to the axons and hence were likely to be intrafascicular oligodendrocytes (Fig. 9A). To confirm this, we double-labeled sections for NDRG1 and an astrocyte marker (glial fibrillary acidic protein; GFAP), a neuronal marker (NeuN), and an oligodendrocyte marker (APC). NDRG1-positive cells also expressed APC (Figs. 9B and C), but not GFAP or NeuN (data not shown), demonstrating that they are oligodendrocytes. In regions that contained fewer myelinated axons, robust NDRG1 immunoreactivity was seen in oligodendrocytes cell bodies and processes (Figs. 9E and F). To determine whether primate oligodendrocytes express NDRG1, we immunostained sections of the medulla from a rhesus monkey (*Macaca mulatta*). NDRG1-positive cells resembling oligodendrocytes were found in white matter tracts (Fig. 9D) as well as in gray matter (data not shown). Because the anti-APC antibody did not cross react on these sections, we were unable to demonstrate more directly that these NDRG1-postive cells were oligodendrocytes.

To evaluate these findings further, we examined NDRG1 mRNA expression in developing rat brain. As shown in Fig. 10A, NDRG1 mRNA increased from P14 to P30, in parallel with MBP mRNA; this corresponds with the expected developmental increase of myelin-related mRNAs (Scherer et al., 1994). We compared this pattern of expression to that in myelin-deficient rats, which have a point mutation in the gene encoding proteolipid protein (Boison and Stoffel, 1989); this results in oligodendrocyte cell death and decreased levels of myelin-related mRNAs (Scherer et al., 1995). The level of NDRG1 mRNA in the brains of myelin-deficient rats was diminished compared to that of their wild-type littermates, but not as marked as that of MBP (Fig. 10B). As in wild-type rats, all NDRG1-positive cells in myelin-deficient spinal cords were colabeled with the oligodendrocyte markers MAG and APC (data not shown).

Discussion

Our results demonstrate that myelinating Schwann cells, but not sensory or motor neurons, express NDRG1. Thus, protein-truncating NDRG1 mutations in CMT4D/HMSNL are probably deleterious to myelinating Schwann cells, thereby causing demyelination and subsequent axonal degeneration. Similarly, in the CNS, NDRG1 appears to be solely expressed by oligodendrocytes so that the loss of NDRG1 expression in oligodendro-

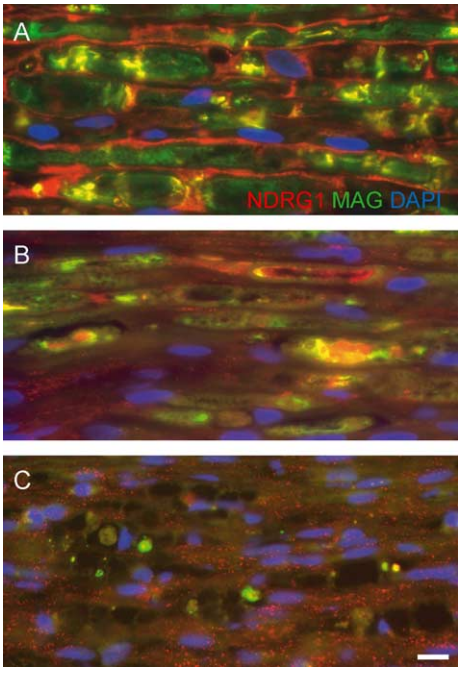

Fig. 8. NDRG1 protein disappears during Wallerian degeneration. These are images of sections of the distal nerve stump of adult rat sciatic nerves, 4 days (A), 12 days (B), and 58 days (C) posttransection, double labeled with a rabbit antiserum against NDRG1 (red) and a monoclonal antibody against MAG (green); DAPI (blue) is a nuclear counterstain. At 4 days, NDRG1 and MAG staining are still found in the outer or abaxonal and inner or adaxonal regions, respectively, and they overlap in incisures (yellow). At 12 days, the architecture of myelin sheaths is largely obliterated. There is much less NDRG1 and MAG immunoreactivity, which partially overlap in large blobs. At 58 days, there are small "speckles" of NDRG1 immunoreactivity in Schwann cells and scattered small blobs of MAG immunoreactivity in macrophages. Scale bar: 10 μm.

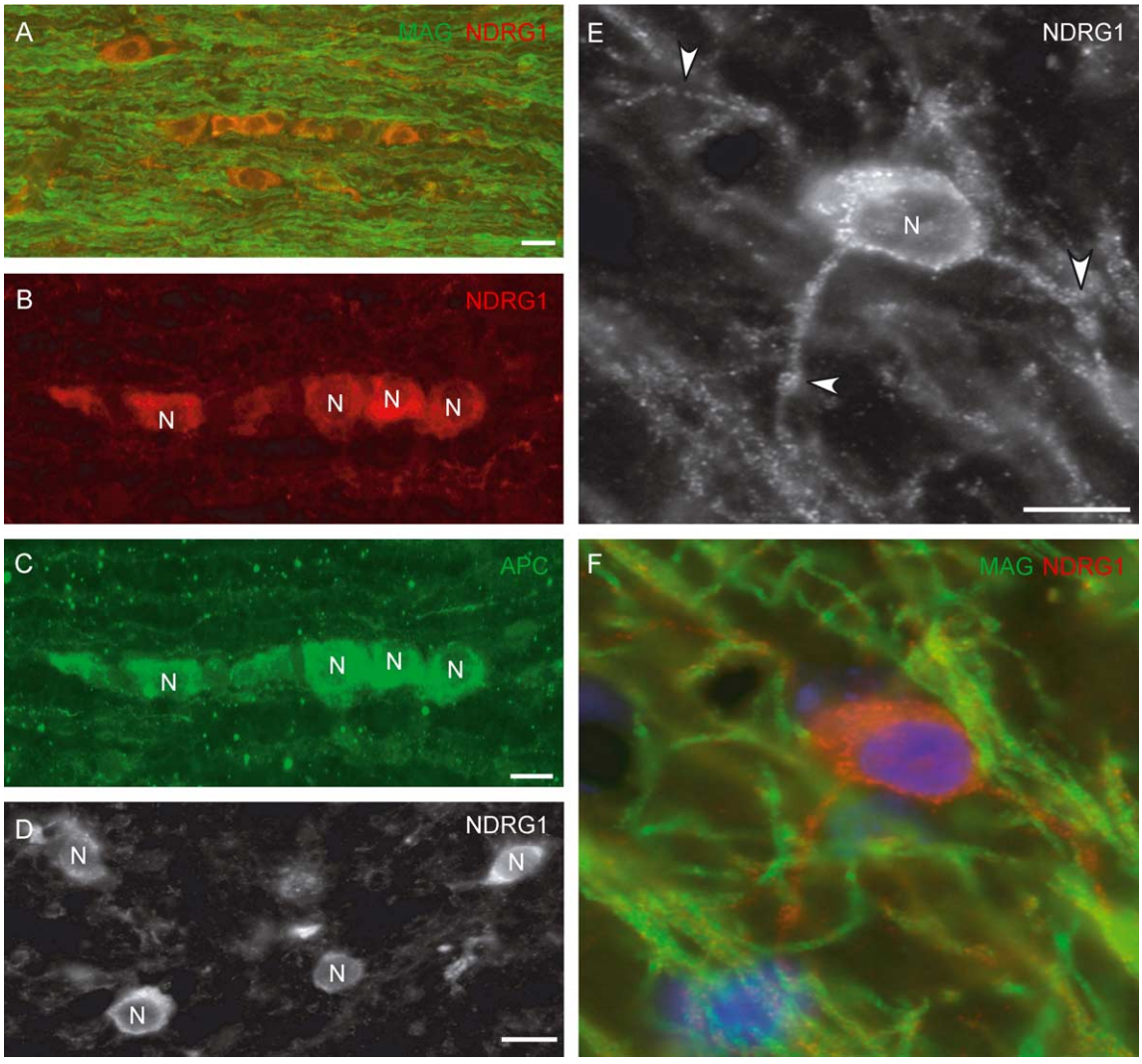

Fig. 9. Oligodendrocytes express NDRG1. These are images of longitudinal sections of adult rat spinal cord (A–C), monkey medulla (D), and mouse cortex (E and F), double labeled with a rabbit antiserum to NDRG1 (red) and monoclonal antibodies (green) against MAG (A and F) or APC (C). NDRG1 is found in intrafascicular oligodendrocytes (A and B) and colocalizes with APC (C). NDRG1 is found mainly in the cytoplasm, including the processes (arrowheads) of oligodendrocytes (E and F). Scale bars: 10 μm.

cytes would likely account for any CNS manifestations of CMT4D. Unlike other causative proteins of inherited demyelinating neuropathies like PMP22, P0, connexin32 (Cx32), and periaxin (Arroyo and Scherer, 2000; Scherer and Arroyo, 2002), NDRG1 is cytosolic, suggesting that the loss of NDRG1 causes demyelination by a distinct pathway (Suter and Scherer, 2003).

This is the first report to evaluate the localization and regulation of NDRG1 in the PNS. NDRG1 is mainly localized to the cytoplasm of myelinating Schwann cells and disappears after axotomy. It has been suggested that NDRG1 is associated with adhering junctions in other cell types (Lachat et al., 2002). The localization of NDRG1 does overlap that of E-cadherin, which is found in the adhering junctions of incisures and paranodes (Fannon and Colman, 1996; Young et al., 2002). However, the localization of NDRG1 in incisures and paranodes may be more apparent than real, as these structures contain small amounts of cytoplasm (Scherer and Arroyo, 2002). The prominent cytoplasmic staining of oligodendrocytes also supports the idea that NDRG1 is not strictly associated with adhering junctions, which are not found in mature oligodendrocytes (Arroyo and Scherer, 2000).

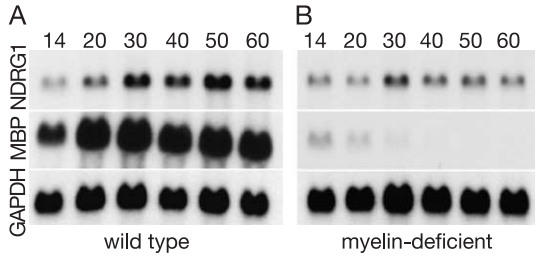

Fig. 10. Expression of NDRG1 mRNA in normal and myelin-deficient rat brain. Each lane contains 10 μg of total RNA isolated from brains of myelin-deficient rats or their wild-type littermates at the indicated postnatal ages. The blots were hybridized together, sequentially, with radiolabeled cDNA probes for NDRG1, GAPDH, and MBP and exposed to film 14 days, 4 h, and 4 h, respectively.

NDRG1 mRNA expression is regulated similar to myelin proteins during nerve development and after nerve injury. A large number of myelin-related mRNAs show remarkably similar patterns of expression, including P0, PMP22, MBP, MAG, Cx32, periaxin, and Krox20/EGR2 (Kamholz et al., 2000; Scherer and Salzer, 2001). Thus, it is likely that a specific set of transcription factors regulates these genes in common, including EGR2 and POU-domain transcription factors (Jaegle et al., 2003; Nagarajan et al., 2001). However, at least two genes that cause a demyelinating neuropathy—MTMR2 (Bolino et al., 2002) and LITAF (Street et al., 2003)—do not appear to be regulated in this manner.

The phenotype of individuals who have CMT4D includes subclinical evidence of central conduction slowing (Kalaydjieva et al., 1998). This finding suggests that oligodendrocytes are also affected by a loss of NDRG1. In keeping with this possibility, we show that NDRG1 is localized to the cytoplasm of oligodendrocytes, and that NDRG1 mRNA levels are reduced in a dysmyelinating mutant. These findings are reminiscent of those in CMT1X, which is caused by mutations in the gene that encodes the gap junction protein Cx32. Cx32 is expressed by oligodendrocytes, but by few if any neurons (Scherer et al., 1995). Although most individuals with CMT1X do not have overt CNS symptoms or findings, subclinical slowing of the BAEPs is common (Nicholson et al., 1998), and a few individuals have striking, transient neurological deficits that are associated with acute changes in their brains (Taylor et al., 2003).

In conclusion, the specific localization and regulated expression of NDRG1 in myelinating Schwann cells strongly suggest that it plays a unique role in these cells and probably also in oligodendrocytes. The precise role of NDRG1 in myelinating glial cells, and indeed its functional role in any cell type, remains to be determined.

Acknowledgments

We thank Dr. Ned Mantei for critically reading the manuscript, Drs. S. Fuller, H.P. Hauri, E. Ehler, and J. Gruenberg for antibodies, Dr. Judy Grinspan for myelin-deficient rats, Dr. Alex Gow for sections of monkey medulla, and Susan Shumas for excellent technical assistance. This work was supported by the Swiss National Science Foundation, the Swiss Muscle Disease Foundation, the National Center of Competence in Research "Neural Plasticity and Repair," and the Swiss Bundesamt for Science related to the Commission of the European Communities, specific RTD program "Quality of Life and Management of Living Ressources," QLK6-CT-2000-00179 (to US) and the NIH RO1 NS42878 and NS43174 (to SSS).

References

Adlkofer, K., Martini, R., Aguzzi, A., Zielasek, J., Toyka, K.V., Suter, U., 1995. Hypermyelination and demyelinating peripheral neuropathy in Pmp22-deficient mice. Nat. Genet. 11, 274–280.

Adlkofer, K., Frei, R., Neuberg, D.H., Zielasek, J., Toyka, K.V., Suter, U., 1997. Heterozygous peripheral myelin protein 22-deficient mice are affected by a progressive demyelinating tomaculous neuropathy. J. Neurosci. 17, 4662–4671.

Agarwala, K.L., Kokame, K., Kato, H., Miyata, T., 2000. Phosphorylation of RTP, an ER stress-responsive cytoplasmic protein. Biochem. Biophys. Res. Commun. 272, 641–647.

Arroyo, E.J., Scherer, S.S., 2000. On the molecular architecture of myelinated fibers. Histochem. Cell Biol. 113, 1–18.

Baethmann, M., Gohlich-Ratmann, G., Schroder, J.M., Kalaydjieva, L., Voit, T., 1998. HMSNL in a 13-year-old Bulgarian girl. Neuromuscular Disord. 8, 90–94.

Bandyopadhyay, S., Pai, S.K., Gross, S.C., Hirota, S., Hosobe, S., Miura, K., Saito, K., Commes, T., Hayashi, S., Watabe, M., Watabe, K., 2003. The *Drg-1* gene suppresses tumor metastasis in prostate cancer. Cancer Res. 63, 1731–1736.

Berger, P., Young, P., Suter, U., 2002a. Molecular cell biology of Charcot–Marie–Tooth disease. Neurogenetics 4, 1–15.

Berger, P., Bonneick, S., Willi, S., Wymann, M., Suter, U., 2002b. Loss of phosphatase activity in myotubularin-related protein 2 is associated with Charcot–Marie–Tooth disease type 4B1. Hum. Mol. Genet. 11, 1569–1579.

Boerkoel, C.F., Takashima, H., Garcia, C.A., Olney, R.K., Johnson, J., Berry, K., Russo, P., Kennedy, S., Teebi, A.S., Scavina, M., Williams, L.L., Mancias, P., Butler, I.J., Krajewski, K., Shy, M., Lupski, J.R., 2002. Charcot–Marie–Tooth disease and related neuropathies: mutation distribution and genotype-phenotype correlation. Ann. Neurol. 51, 190–201.

Boison, D., Stoffel, W., 1989. Myelin-deficient rat: a point mutation in exon III (A–C, Thr75–Pro) of the myelin proteolipid protein causes dysmyelination and oligodendrocyte death. EMBO J. 8, 3295–3302.

Bolino, A., Marigo, V., Ferrera, F., Loader, J., Romio, L., Leoni, A., Di Duca, M., Cinti, R., Cecchi, C., Feltri, M.L., Wrabetz, L., Ravazzolo, R., Monaco, A.P., 2002. Molecular characterization and expression analysis of Mtmr2, mouse homologue of MTMR2, the myotubularin-related 2 gene, mutated in CMT4B. Gene 283, 17–26.

Butinar, D., Zidar, J., Leonardis, L., Popovic, M., Kalaydjieva, L., Angelicheva, D., Sininger, Y., Keats, B., Starr, A., 1999. Hereditary auditory, vestibular, motor, and sensory neuropathy in a Slovenian Roma (Gypsy) kindred. Ann. Neurol. 46, 36–44.

Chirgwin, J.M., Przybyla, A.E., MacDonald, R.J., Rutter, W.J., 1979. Isolation of biologically active ribonucleic acid from sources enriched in ribonuclease. Biochemistry 18, 5294–5299.

Dyck, P.J., Lambert, E.H., 1968a. Lower motor and primary sensory neuron diseases with peroneal muscular atrophy. II. Neurologic, genetic, and electrophysiologic findings in various neuronal degenerations. Arch. Neurol. 18, 619–625.

Dyck, P.J., Lambert, E.H., 1968b. Lower motor and primary sensory neuron diseases with peroneal muscular atrophy. I. Neurologic, genetic, and electrophysiologic findings in hereditary polyneuropathies. Arch. Neurol. 18, 603–618.

Dyck, P.J., Chance, P., Lebo, R., Carney, J.A., 1993. Hereditary motor and sensory neuropathies. In: Dyck, P.J., Thomas, P.K., Grffin, J.W., Low, P.A., Poduslo, J.F. (Eds.), Peripheral Neuropathy, 3rd ed. Saunders, Philadelphia, pp. 1094–1136.

Fannon, A.M., Colman, D.R., 1996. A model for central synaptic junctional complex formation based on the differential adhesive specificities of the cadherins. Neuron 17, 423–434.

Fort, P., Marty, L., Piechaczyk, M., el Sabrouty, S., Dani, C., Jeanteur, P., Blanchard, J.M., 1985. Various rat adult tissues express only one major mRNA species from the glyceraldehyde-3-phosphate-dehydrogenase multigenic family. Nucleic Acids Res. 13, 1431–1442.

Guan, R.J., Ford, H.L., Fu, Y., Li, Y., Shaw, L.M., Pardee, A.B., 2000. Drg-1 as a differentiation-related, putative metastatic suppressor gene in human colon cancer. Cancer Res. 60, 749–755.

Jaegle, M., Ghazvini, M., Mandemakers, W., Piirsoo, M., Driegen, S., Levavasseur, F., Raghoenath, S., Grosveld, F., Meijer, D., 2003. The POU proteins Brn-2 and Oct-6 share important functions in Schwann cell development. Genes Dev. 17, 1380–1391.

Kalaydjieva, L., Hallmayer, J., Chandler, D., Savov, A., Nikolova, A., Angelicheva, D., King, R.H., Ishpekova, B., Honeyman, K., Calafell, F., Shmarov, A., Petrova, J., Turnev, I., Hristova, A., Moskov, M., Stancheva, S., Petkova, I., Bittles, A.H., Georgieva, V., Middleton, L., Thomas, P.K., 1996. Gene mapping in Gypsies identifies a novel

demyelinating neuropathy on chromosome 8q24. Nat. Genet. 14, 214–217.
Kalaydjieva, L., Nikolova, A., Turnev, I., Petrova, J., Hristova, A., Ishpekova, B., Petkova, I., Shmarov, A., Stancheva, S., Middleton, L., Merlini, L., Trogu, A., Muddle, J.R., King, R.H., Thomas, P.K., 1998. Hereditary motor and sensory neuropathy-Lom, a novel demyelinating neuropathy associated with deafness in gypsies. Clinical, electrophysiological and nerve biopsy findings. Brain 121 (Pt 3), 399–408.
Kalaydjieva, L., Gresham, D., Gooding, R., Heather, L., Baas, F., de Jonge, R., Blechschmidt, K., Angelicheva, D., Chandler, D., Worsley, P., Rosenthal, A., King, R.H., Thomas, P.K., 2000. N-myc downstream-regulated gene 1 is mutated in hereditary motor and sensory neuropathy-Lom. Am. J. Hum. Genet. 67, 47–58.
Kamholz, J., Menichella, D., Jani, A., Garbern, J., Lewis, R.A., Krajewski, K.M., Lilien, J., Scherer, S.S., Shy, M.E., 2000. Charcot–Marie–Tooth disease type 1: molecular pathogenesis to gene therapy. Brain 123, 222–233.
Kleopa, K.A., Scherer, S.S., 2002. Inherited neuropathies. Neurol. Clin. 20, 679–709.
Kokame, K., Kato, H., Miyata, T., 1996. Homocysteine-respondent genes in vascular endothelial cells identified by differential display analysis, GRP78/BiP and novel genes. J. Biol. Chem. 271, 29659–29665.
Kurdistani, S.K., Arizti, P., Reimer, C.L., Sugrue, M.M., Aaronson, S.A., Lee, S.W., 1998. Inhibition of tumor cell growth by RTP/rit42 and its responsiveness to p53 and DNA damage. Cancer Res. 58, 4439–4444.
Lachat, P., Shaw, P., Gebhard, S., van Belzen, N., Chaubert, P., Bosman, F.T., 2002. Expression of NDRG1, a differentiation-related gene, in human tissues. Histochem. Cell Biol. 118, 399–408.
Lee, V., Wu, H.L., Schlaepfer, W.W., 1982. Monoclonal antibodies recognize individual neurofilament triplet proteins. Proc. Natl. Acad. Sci. U. S. A. 79, 6089–6092.
Lemke, G., Axel, R., 1985. Isolation and sequence of a cDNA encoding the major structural protein of peripheral myelin. Cell 40, 501–508.
Magyar, J.P., Martini, R., Ruelicke, T., Aguzzi, A., Adlkofer, K., Dembic, Z., Zielasek, J., Toyka, K.V., Suter, U., 1996. Impaired differentiation of Schwann cells in transgenic mice with increased PMP22 gene dosage. J. Neurosci. 16, 5351–5360.
Maier, M., Berger, P., Nave, K.A., Suter, U., 2002. Identification of the regulatory region of the peripheral myelin protein 22 (PMP22) gene that directs temporal and spatial expression in development and regeneration of peripheral nerves. Mol. Cell. Neurosci. 20, 93–109.
Merlini, L., Villanova, M., Sabatelli, P., Trogu, A., Malandrini, A., Yanakiev, P., Maraldi, N.M., Kalaydjieva, L., 1998. Hereditary motor and sensory neuropathy Lom type in an Italian Gypsy family. Neuromuscular Disord. 8, 182–185.
Naef, R., Adlkofer, K., Lescher, B., Suter, U., 1997. Aberrant protein trafficking in Trembler suggests a disease mechanism for hereditary human peripheral neuropathies. Mol. Cell. Neurosci. 9, 13–25.
Nagarajan, R., Svaren, J., Le, N., Araki, T., Watson, M., Milbrandt, J., 2001. EGR2 mutations in inherited neuropathies dominant-negatively inhibit myelin gene expression. Neuron 30, 355–368.
Nicholson, G.A., Yeung, L., Corbett, A., 1998. Efficient neurophysiologic selection of X-linked Charcot–Marie–Tooth families: ten novel mutations. Neurology 51, 1412–1416.
Piquemal, D., Joulia, D., Balaguer, P., Basset, A., Marti, J., Commes, T., 1999. Differential expression of the RTP/Drg1/Ndr1 gene product in proliferating and growth arrested cells. Biochim. Biophys. Acta 1450, 364–373.
Qu, X., Zhai, Y., Wei, H., Zhang, C., Xing, G., Yu, Y., He, F., 2002. Characterization and expression of three novel differentiation-related genes belong to the human NDRG gene family. Mol. Cell. Biochem. 229, 35–44.
Sambrook, J., Fritsch, E.F., Maniatis, T., 1989. Molecular Cloning: A Laboratory Manual, 2nd ed. Cold Spring Harbor Laboratory Press, pp. 7.37–7.52.
Scherer, S.S., Arroyo, E.J., 2002. Recent progress on the molecular organization of myelinated axons. J. Peripher. Nerv. Syst. 7, 1–12.
Scherer, S.S., Salzer, J., 2001. Axon–Schwann cell interactions in peripheral nerve degeneration and regeneration. In: Jessen, K.R., Richardson, W.D. (Eds.), Glial Cell Development, 2nd ed. Oxford Univ. Press, Oxford, pp. 299–330.
Scherer, S.S., Braun, P.E., Grinspan, J., Collarini, E., Wang, D.Y., Kamholz, J., 1994. Differential regulation of the 2′,3′-cyclic nucleotide 3′ phosphodiesterase gene during oligodendrocyte development. Neuron 12, 1363–1375.
Scherer, S.S., Deschenes, S.M., Xu, Y.-T., Grinspan, J.B., Fischbeck, K.H., Paul, D.L., 1995. Connexin32 is a myelin-related protein in the PNS and CNS. J. Neurosci. Res. 15, 8281–8294.
Segawa, T., Nau, M.E., Xu, L.L., Chilukuri, R.N., Makarem, M., Zhang, W., Petrovics, G., Sesterhenn, I.A., McLeod, D.G., Moul, J.W., Vahey, M., Srivastava, S., 2002. Androgen-induced expression of endoplasmic reticulum (ER) stress response genes in prostate cancer cells. Oncogene 21, 8749–8758.
Shaw, E., McCue, L.A., Lawrence, C.E., Dordick, J.S., 2002. Identification of a novel class in the alpha/beta hydrolase fold superfamily: the N-myc differentiation-related proteins. Proteins 47, 163–168.
Shimono, A., Okuda, T., Kondoh, H., 1999. N-myc-dependent repression of ndr1, a gene identified by direct subtraction of whole mouse embryo cDNAs between wild type and N-myc mutant. Mech. Dev. 83, 39–52.
Snipes, G.J., Suter, U., Welcher, A.A., Shooter, E.M., 1992. Characterization of a novel peripheral nervous system myelin protein (PMP-22/SR13). J. Cell Biol. 117, 225–238.
Street, V.A., Bennett, C.L., Goldy, J.D., Shirk, A.J., Kleopa, K.A., Tempel, B.L., Lipe, H.P., Scherer, S.S., Bird, T.D., Chance, P.F., 2003. Mutation of a putative protein degradation gene LITAF/SIMPLE in Charcot–Marie–Tooth disease 1C. Neurology 60, 22–26.
Suter, U., Scherer, S.S., 2003. Disease mechanisms in inherited neuropathies. Nat. Rev. Neurosci. 4, 714–726.
Suter, U., Moskow, J.J., Welcher, A.A., Snipes, G.J., Kosaras, B., Sidman, R.L., Buchberg, A.M., Shooter, E.M., 1992. A leucine-to-proline mutation in the putative first transmembrane domain of the 22-kDa peripheral myelin protein in the trembler-J mouse. Proc. Natl. Acad. Sci. U. S. A. 89, 4382–4386.
Taylor, V., Welcher, A.A., Program, A.E., Suter, U., 1995. Epithelial membrane protein-1, peripheral myelin protein 22, and lens membrane protein 20 define a novel gene family. J. Biol. Chem. 270, 28824–28833.
Taylor, R.A., Simon, E.M., Marks, H.G., Scherer, S.S., 2003. The CNS phenotype of X-linked Charcot–Marie–Tooth disease: more than a peripheral problem. Neurology 61, 1475–1478.
Tobler, A.R., Notterpek, L., Naef, R., Taylor, V., Suter, U., Shooter, E.M., 1999. Transport of Trembler-J mutant peripheral myelin protein 22 is blocked in the intermediate compartment and affects the transport of the wild-type protein by direct interaction. J. Neurosci. 19, 2027–2036.
Ulrix, W., Swinnen, J.V., Heyns, W., Verhoeven, G., 1999. The differentiation-related gene 1, Drg1, is markedly upregulated by androgens in LNCaP prostatic adenocarcinoma cells. FEBS Lett. 455, 23–26.
van Belzen, N., Dinjens, W.N., Diesveld, M.P., Groen, N.A., van der Made, A.C., Nozawa, Y., Vlietstra, R., Trapman, J., Bosman, F.T., 1997. A novel gene which is up-regulated during colon epithelial cell differentiation and down-regulated in colorectal neoplasms. Lab. Invest. 77, 85–92.
Young, P., Boussadia, O., Berger, P., Leone, D.P., Charnay, P., Kemler, R., Suter, U., 2002. E-cadherin is required for the correct formation of autotypic adherens junctions of the outer mesaxon but not for the integrity of myelinated fibers of peripheral nerves. Mol. Cell. Neurosci. 21, 341–351.
Zhou, D., Salnikow, K., Costa, M., 1998. Cap43, a novel gene specifically induced by Ni2+ compounds. Cancer Res. 58, 2182–2189.
Zoroddu, M.A., Kowalik-Jankowska, T., Kozlowski, H., Salnikow, K., Costa, M., 2001. Ni(II) and Cu(II) binding with a 14-aminoacid sequence of Cap43 protein, TRSRSHTSEGTRSR. J. Inorg. Biochem. 84, 47–54.